



Ritz Variational Method for the Analysis of Thin Rectangular Plate Bending Problems with Adjacent Edges Clamped and Simply Supported Using the Superposition of Trigonometric Series and Polynomial Basis Functions

Charles Chinwuba Ike

Department of Civil Engineering, Enugu State University of Science and Technology, Agbani, 402004, Enugu State, Nigeria

PAPER INFO

Paper history (8pt)

Received: 10/04/2024

Revised: 13/06/2024

Accepted: 25/06/2024

Keywords:

Bending moment

Center deflection

Kirchhoff plate

Ritz variational functional

Superposition of trigonometric series and polynomial basis functions



Copyright: ©2024 by the authors.
Submitted for possible open-access publication under the terms and conditions of the Creative Commons Attribution (CC BY-NC 4.0) license.
<https://creativecommons.org/licenses/by-nc/4.0/>

ABSTRACT

This paper attempts to obtain bending solutions to plates under uniformly distributed and hydrostatic load distributions using Ritz variational methods and basis functions that are found by superposing trigonometric series and third-degree polynomials. Two cases of boundary conditions were considered. In one case, three edges were simply supported and the fourth edge ($x = a$) was clamped (SSCS thin plate). In the second case, the adjacent edges ($y = b, x = a$) were clamped and the other edges ($x = 0, y = 0$) were simply supported (SSCS thin plate). This work presents first principles, rigorous derivation of the governing Ritz variational functional and the displacement basis functions for the boundary conditions investigated. The solution is presented in analytical form. The obtained results are compared with previous results obtained using Levy series and Ritz methods and found to be in close agreement. The disadvantage of the method is the associated computational rigour, but the benefit is the accuracy of the results. Comparisons of the present results for center deflections and center bending moments with results in the literature show that there is negligible difference. Double series expressions were found for deflections and bending moments for the plate bending problems solved. Evaluation of the double series expressions at the plate center gave center deflection results that differed from the exact solutions by -0.215% for $a/b = 2$ to 0.29% for $a/b = 1.1$ for uniformly loaded thin plates with three simply supported edges and one clamped edge (SSSC). The differences in the center bending moments M_{xx} were found to vary from 2.34% for $a/b = 2$ to 1.19% for $a/b = 1.1$. In general, the present results yielded reasonably accurate solutions for the plate bending problems studied.

1. Introduction

Plates are idealizations of structural members of building, aerospace, mechanical, naval and foundation structures which have transverse dimensions that are much smaller than their in-plane dimensions. They are thus

* Corresponding author. Tel.: +234-8033101883.
E-mail address: charles.ike@esut.edu.ng

spatial structures that may be subjected to transverse static, dynamic forces or in-plane loads. They can thus respond to loading by transverse static flexure, dynamic flexure or in-plane compression. According to their materials, they can be classified as homogeneous or nonhomogeneous, isotropic or non-isotropic, elastic or non-elastic. They may also be made of composite, laminated or functionally graded materials (FGM). Their surfaces may be flat or curved. Based on their in-plane shapes, they may be called rectangular, polygonal, circular, rhombic, skewed, elliptical, quadrilateral, oval, etc.

Plates with disturbed (D) regions at which a considerable disturbance of the contour lines of the flexural stresses, leading to a severe concentration of stress at these regions have been studied and present more complex problems than D-beams which were studied by Shakir and Hanoon (2023, 2024). D-regions occur at the supports, pile caps, non-prismatic plates and can be induced by abrupt changes in geometry, such as openings, in the plate domain (Shakir and Yahya, 2024; Shakir and Farooq alghazali, 2023).

The Bernoulli regions (B-regions) are regions of the plate with no significant turbulence in stress contour lines. The flexural stress theory can then be applied in B-regions (Shakir and Alliwe, 2020; Shakir and Hanoon, 2024).

Plate behaviour depends on the ratio of their least in-plane dimensions, a , to thickness, h ; and accordingly they have been classified as thin plates, moderately thick plates, and thick plates.

For thin plates, $a/h \geq 20$, for moderately thick plates $10 < a/h < 20$, for thick plates, $a/h < 10$.

Thin plate theory was originally derived by Kirchhoff based on the hypothesis that the cross-sectional planes that are initially normal to the middle surface remain normal to the middle surface after deformation.

The middle surface is the reference surface. The implication of the normality hypothesis is that shear stresses that could introduce distortions of the plane cross-section are disregarded in the formulation and this restricts the scope of the thin plate theory to cases where such shear stresses are insignificant. Thus, the Kirchhoff plate theory (KPT) is scoped to thin plates for which $h/a \leq 0.05$.

When shear deformation effects begin to exert appreciable effects on the plate behaviour as noticed in thick and moderately thick plates, and laminated and composite plates, the normality hypothesis no longer applies because the plane cross-sections experience distortion during bending and can no longer be normal to the middle surface during and after deformation (Koc, 2023). The KPT gives inaccurate results for the bending, buckling and dynamic analysis of moderately thick and thick plates.

Research efforts directed at offering improvements to KPT such as to take shear deformations into account led various scholars to develop several theories, models and formulations of plates. Reissner (1945) used a stress-based method to derive Reissner plate theory that considered shear deformation effects, resulting in a sixth order shear deformation plate theory. Mindlin (1951) used a displacement based approach to derive the Mindlin plate theory as a first order shear deformation theory that considered shear deformation effects by relaxing the normality hypothesis. Other shear deformation theories of plates were formulated using various assumptions about the kinematics of displacement by Reddy (1984); Ghugal and Gajbhiye (2016); Ghugal and Sayyad (2010); Soltani et al (2019) and Nareen and Shimpi (2015).

The focus of this work is on thin plates flexural analysis using a novel solution method which assumes the basis function to be a combination of sine series and polynomial functions in the principle of minimization of the Ritz energy functional.

The solution methods for plate analysis are categorized as approximate (numerical) methods, and exact (analytical) methods. The approximate (numerical) methods are the:

- ❖ finite difference method (FDM)
- ❖ finite element method (FEM) (Karttunen et al, 2017)
- ❖ collocation method (Guo et al, 2019)
- ❖ Ritz variational method (RVM) (Lytvyn et al, 2018)
- ❖ Galerkin variational method (GVM)
- ❖ Method of Weighted Residuals (MWR), Meshless methods (Du et al, 2022)

Analytical methods of solving plate bending problems are scarce. The reason is that the mathematical solutions of the governing partial differential equations for plates is very difficult to obtain except for the cases of plates with two opposite simply supported edges, which are solved using the classical Levy semi-inverse single trigonometric series method.

For rectangular thin plates with two opposite edges simply supported, the analytical methods used include semi-inverse superposition method, series method (Fogang, 2023); integral transform methods; symplectic elasticity method (Shuang, 2007; Ma, 2008; Lim et al, 2007; Zhong and Li, 2009; Wang et al, 2016; Su et al,

2023; Zheng et al, 2021).

Rezaiee-Pajand and Karkon (2014) presented hybrid stress and analytical functions for the finite element analysis of thin plates in bending. Their work presented two efficient plate bending finite elements: namely, triangular element (THS) and a quadrilateral element (QHS) with 9 and 12 degrees of freedom respectively. Formulation of the elements utilized hybrid variational principle and analytical homogeneous solution of thin plate equation. They verified the high accuracy of the elements.

Rouzegar and Abdoli-Sharifpoor (2015) derived a finite element formulation based on two-variable refined plate theory (RPT) for the bending analysis of isotropic and orthotropic plates. Their work is applicable to thin and thick plate and satisfies the transverse shear stress free boundary conditions at the plate surfaces.

The focus of this work is thin plate bending analysis; which has been studied in the literature using various methods. Galerkin-Vlasov method has been applied for the flexural analysis of rectangular thin plate bending problems by Osadebe et al (2016). Kantorovich methods and various variants of Kantorovich methodology using Vlasov and Ritz refinements have been used for obtaining accurate solutions to flexural analysis of rectangular Kirchhoff plate bending problems by Ike (2017c) and Onah et al (2017). Ritz variational method has been effectively used for accurate solutions of plate bending problems by Ike (2018), Nwoji et al (2018c).

Gao et al (2019) presented accurate solutions for flexural analysis of SCSF and CCCF rectangular thin plates subjected to hydrostatic loads. Razaiee-Pajand and Karkon (2014) presented analytical solutions for thin plate bending problems. Oba et al (2018) used energy minimization method to obtain accurate solutions to thin rectangular plate bending problems. Ibearugbulam et al (2019) used Taylor-Mclaurin series shape functions that were made to satisfy simply supported boundary conditions to solve thin rectangular SSSS plate bending problems.

Li et al (2015) used a novel symplectic superposition method to derive a unified analytical solution to both static flexure and natural vibrations problems of rectangular thin plates for cases of corner-supported plates. Their symplectic superposition method transformed the problems into the Hamiltonian system, yielding accurate results via systematic rigorous approach. The major merit is the extensive scope of application since it needs no prior determined shape functions, which is a departure from commonly found methods. Illustrative examples in their study validated their results and gave new results for previously unsolved problems. Their study offered benchmark analytic solutions, and was effective and accurate.

Wang et al (2016) used symplectic superposition method to derive new analytical solutions for buckling of rectangular Kirchhoff plates, but did not solve bending problems. Recently, Su et al (2023) used symplectic superposition method to present unified solution for some problems of rectangular plates with four free edges. Fogang (2023) used Fourier series method to solve the bending analysis of isotropic, rectangular Kirchhoff plates under applied bending moments. Ike (2023) used variational Kantorovich-Vlasov method to derive exact mathematical solutions to bending problems of SFrSFr Kirchhoff plates. Ike (2021) used variational Ritz-Kantorovich-Euler-Lagrange method to solve the elastic buckling problems of clamped rectangular thin plates, but did not extend the method to flexural analysis of plate problems.

Ike et al (2020) used Least squares weighted residual methods to obtain elasticity solutions for stresses in rectangular plates subjected to uniaxial parabolically distributed edge loads. Mama, Oguaghamba and Ike (2020) used single finite Fourier sine transform method to obtain exact bending solutions for rectangular Kirchhoff plate with opposite edges simply supported, other edges clamped, which is under triangular load distribution.

Ike (2021) used generalized integral transform method (GITM) for the flexural analysis of rectangular thin plates with clamped boundaries and a mixture of clamped and simply supported boundaries; and obtained accurate solutions. Musa et al (2020) applied Ritz method to the flexural analysis of Kirchhoff plates with mixed boundary conditions and supported on inhomogeneous, variable subgrade. Their study presented a systematic means for finding the Ritz basis functions satisfying the geometric boundary conditions for different types of plate edge restraints. They presented illustrative numerical examples to verify the results' accuracy.

Lytvyn et al (2018) presented an algorithm for solving the biharmonic differential equation for clamped plate using the Ritz method, and via explicit splines of degree 5. Xia and Li (2021) used the variational method and R function theory to solve the thin plate bending problem with complex boundary configurations. The R function was used to express the complex area as an implicit function, thus making easier, the determination of trial functions for the complex shape; and ensuring the satisfaction of the complex boundary conditions. This enables the determination of the variational equations of the problem that is solved. Their solutions were validated by numerical solutions of rectangular, and complex shapes that compared favourably with previous solutions in the

literature. Zerfu and Ekaputri (2017) used the principle of minimization of the total energy of a bending plate under applied loads to determine an approximate deflection function for the bending analysis of thin quadrilateral plate. Arnold, Brezzi and Marini (2005) developed locking-free finite elements for moderately thick plates using Discontinuous Galerkin Finite Element Method (DGFEM).

Hansbo and Larson (2017) extended the continuous/discontinuous Galerkin finite element method to the analysis of arbitrarily oriented plates that permit for membrane deformations. They used surface differential calculus to derive Kirchhoff plate models that include in-plane membrane deformations; and finite element method for solving the resulting set of partial differential equations.

Goloskokov and Matrosov (2017) presented the study of structures with non-continuous properties.

This work explores the detailed, systematic solution of the plate bending problems for SSSC and SCCS thin plates using the Ritz variational methodology and basis functions that are derived using a superposition of sine and polynomial functions. The problem was first solved using dimensionless approach by Zhou Ding (1993), who limited his solutions to SSSC thin plate but in this work, the problem is presented in a first principles, rigorous, step by step manner, and extended to plates with adjacent clamped, and simply supported (SCCS) plates. This work is different from Zhou Ding (1993) work because it does not use dimensionless coordinate variable approach in the derivations and implementation.

2. Ritz variational functional (RVF) for Kirchhoff plate bending analysis

2.1. Kirchhoff plate bending problem studied

The Ritz variational functional (RVF) is derived for the thin plate bending problems shown in Figures 1a, 1b and 2.

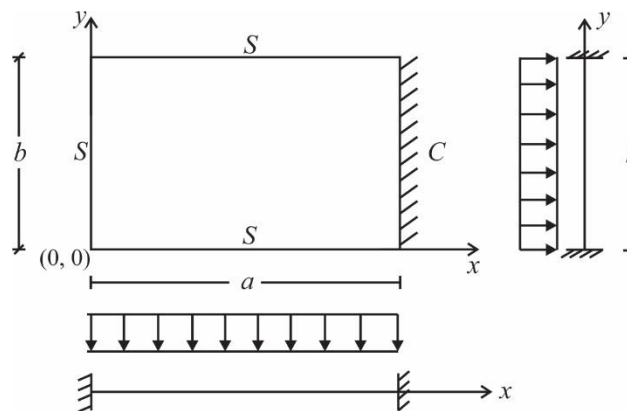


Figure 1a: SSSC thin plate under uniformly distributed load

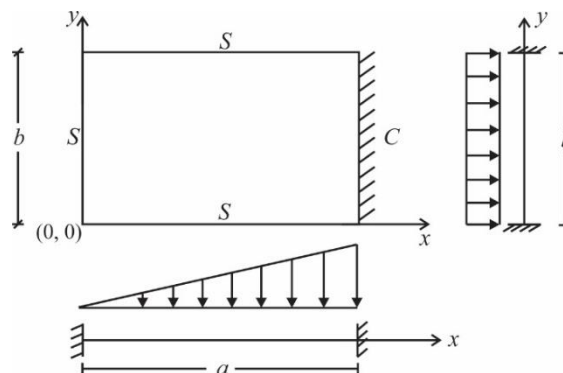


Figure 1b: SSSC thin plate under hydrostatic load distribution

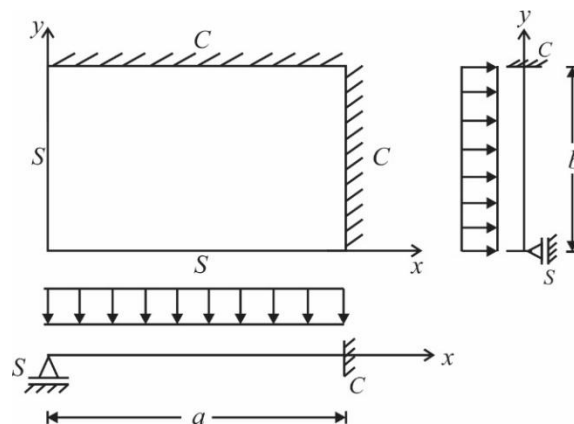


Figure 2: SCCS thin plate under uniformly distributed load

2.2. Theoretical framework of Kirchhoff plate bending theory (KPBT)

The assumptions are (Timoshenko and Woinowsky-Krieger, 1959):

- (i) the mid surface deflection is small compared to the plate thickness, and small deflection theory is used
- (ii) the mid-plane is unstretched prior to flexure
- (iii) stress normal to the mid-plane, σ_z is small relative to other stresses and hence neglected
- (iv) normality hypothesis is valid and transverse shear strains γ_{xz}, γ_{yz} are neglected.

Displacement field components are:

$$u = -z \frac{\partial w(x, y)}{\partial x}, \quad v = -z \frac{\partial w}{\partial y}, \quad w = w(x, y) \tag{1}$$

where u, v, w are the displacement field components in the $x, y,$ and z directions.

The strains are, from the kinematic equations:

$$\begin{aligned} \epsilon_{xx} &= -z \frac{\partial^2 w}{\partial x^2} \\ \epsilon_{yy} &= -z \frac{\partial^2 w}{\partial y^2} \\ \gamma_{xy} &= -2z \frac{\partial^2 w}{\partial x \partial y} \end{aligned} \tag{2}$$

where $\epsilon_{xx}, \epsilon_{yy}$ are normal strains, γ_{xy} is the shear strain

The material constitutive relations for linear elastic, homogeneous, isotropic plate materials are:

$$\begin{aligned} \sigma_{xx} &= \frac{E}{1-\mu^2} (\epsilon_{xx} + \mu \epsilon_{yy}) \\ \sigma_{yy} &= \frac{E}{1-\mu^2} (\epsilon_{yy} + \mu \epsilon_{xx}) \\ \tau_{xy} &= G \gamma_{xy} = \frac{E}{2(1+\mu)} \gamma_{xy} \end{aligned} \tag{3}$$

σ_{xx}, σ_{yy} are normal stresses, τ_{xy} is the shear stress, μ is the Poisson ratio, E is the Young's modulus, G is the shear modulus.

Substituting the expressions for strain-displacement in Equation (3), the stress displacement equations are:

$$\sigma_{xx} = \frac{-Ez}{1-\mu^2} \left(\frac{\partial^2 w}{\partial x^2} + \mu \frac{\partial^2 w}{\partial y^2} \right)$$

$$\sigma_{yy} = \frac{-Ez}{1-\mu^2} \left(\frac{\partial^2 w}{\partial y^2} + \mu \frac{\partial^2 w}{\partial x^2} \right) \tag{4}$$

$$\tau_{xy} = \frac{-Ez}{1+\mu} \frac{\partial^2 w}{\partial x \partial y} = -2Gz \frac{\partial^2 w}{\partial x \partial y}$$

Internal force resultants

The bending moments, M_{xx} , M_{yy} , and twisting moments, M_{xy} are:

$$M_{xx} = \int_{-h/2}^{h/2} \sigma_{xx} z \, dx = -D \left(\frac{\partial^2 w}{dx^2} + \mu \frac{\partial^2 w}{dy^2} \right)$$

$$M_{yy} = \int_{-h/2}^{h/2} \sigma_{yy} z \, dx = -D \left(\frac{\partial^2 w}{dy^2} + \mu \frac{\partial^2 w}{dx^2} \right) \tag{5}$$

$$M_{xy} = - \left(\frac{Gh^3}{6} \right) \frac{\partial^2 w}{\partial x \partial y}$$

where $D = \frac{Eh^3}{12(1-\mu^2)}$ (6)

D is the flexural rigidity.

Strain-Energy, U , of Kirchhoff plate is:

$$U = \frac{1}{2} \int_{-h/2}^{h/2} \int_0^a \int_0^b \left(\sigma_{xx} \epsilon_{xx} + \sigma_{yy} \epsilon_{yy} + \tau_{xy} \gamma_{xy} \right) dx dy dz \tag{7}$$

Substituting the expressions for stresses and strains in Equation (7) gives:

$$U = \frac{1}{2} \int_{-h/2}^{h/2} \int_0^a \int_0^b \left\{ \frac{-Ez}{1-\mu^2} \left(\frac{\partial^2 w}{\partial x^2} + \mu \frac{\partial^2 w}{\partial y^2} \right) \left(-z \frac{\partial^2 w}{\partial x^2} \right) - \frac{Ez}{1-\mu^2} \left(\frac{\partial^2 w}{\partial y^2} + \mu \frac{\partial^2 w}{\partial x^2} \right) \left(-z \frac{\partial^2 w}{\partial y^2} \right) \right. \\ \left. \left(-\frac{Ez}{1+\mu} \frac{\partial^2 w}{\partial x \partial y} \right) \left(-2z \frac{\partial^2 w}{\partial x \partial y} \right) \right\} dx dy dz \tag{8}$$

Simplifying Equation (8) gives:

$$U = \frac{1}{2} \int_{-h/2}^{h/2} \int_0^a \int_0^b \left\{ \frac{Ez^2}{1-\mu^2} \left[\left(\frac{\partial^2 w}{\partial x^2} \right)^2 + \mu \left(\frac{\partial^2 w}{\partial y^2} \right) \left(\frac{\partial^2 w}{\partial x^2} \right) + \left(\frac{\partial^2 w}{\partial y^2} \right)^2 + \mu \left(\frac{\partial^2 w}{\partial x^2} \right) \left(\frac{\partial^2 w}{\partial y^2} \right) \right] \right. \\ \left. + \frac{2Ez^2}{1+\mu} \left(\frac{\partial^2 w}{\partial x \partial y} \right)^2 \right\} dx dy dz \tag{9}$$

Further simplification yields:

$$U = \frac{1}{2} \int_{-h/2}^{h/2} \frac{Ez^2}{1-\mu^2} dz \int_0^a \int_0^b \left[\left(\frac{\partial^2 w}{\partial x^2} \right)^2 + \left(\frac{\partial^2 w}{\partial y^2} \right)^2 + 2\mu \left(\frac{\partial^2 w}{\partial x^2} \right) \left(\frac{\partial^2 w}{\partial y^2} \right) \right] dx dy \\ + \frac{1}{2} \int_{-h/2}^{h/2} \frac{2Ez^2}{1+\mu} dz \int_0^a \int_0^b \left(\frac{\partial^2 w}{\partial x \partial y} \right)^2 dx dy \tag{10}$$

But,

$$\int_{-h/2}^{h/2} \frac{Ez^2}{1-\mu^2} dz = \frac{Eh^2}{12(1-\mu^2)} = D$$

Hence,

$$U = \frac{D}{2} \int_0^a \int_0^b \left(\left(\frac{\partial^2 w}{\partial x^2} + \frac{\partial^2 w}{\partial y^2} \right)^2 - 2(1-\mu) \left(\frac{\partial^2 w}{\partial x^2} \frac{\partial^2 w}{\partial y^2} - \left(\frac{\partial^2 w}{\partial x \partial y} \right)^2 \right) \right) dx dy \quad (11)$$

Alternatively,

$$U = \frac{D}{2} \int_0^a \int_0^b \left((\nabla^2 w)^2 - 2(1-\mu) (w_{xx} w_{yy} - (w_{xy})^2) \right) dx dy \quad (12)$$

$$\text{where } \nabla^2 = \frac{\partial^2}{\partial x^2} + \frac{\partial^2}{\partial y^2}, \quad w_{xx} = \frac{\partial^2 w}{\partial x^2}, \quad w_{yy} = \frac{\partial^2 w}{\partial y^2}, \quad w_{xy} = \frac{\partial^2 w}{\partial x \partial y} \quad (13)$$

The work potential, W_p , due to the applied load $q(x, y)$ is:

$$W_p = \int_0^a \int_0^b q(x, y) w(x, y) dx dy \quad (14)$$

Total potential energy functional Π

The total potential energy functional, Π is:

$$\Pi = U - W_p \quad (15)$$

Then,

$$\Pi = \frac{D}{2} \int_0^a \int_0^b \left((\nabla^2 w)^2 - 2(1-\mu) (w_{xx} w_{yy} - w_{xy}^2) \right) dx dy - \int_0^a \int_0^b q(x, y) w(x, y) dx dy \quad (16)$$

In the method adopted, $w(x, y)$ is expressed in the form of linearly independent functions $F_m(x)$ and $G_n(y)$ as follows:

$$w(x, y) = \sum_{m,n} A_{mn} F_m(x) G_n(y) \quad (17)$$

where A_{mn} are amplitude parameters of $w(x, y)$ and $F_m(x)$ and $G_n(y)$ are expressed using superposed sine and polynomial functions such that relevant boundary conditions are satisfied.

The functional Π then becomes expressible in terms of A_{mn} , and the work aims to minimize Π with respect to A_{mn} in order to achieve equilibrium of the plate system. This principle of minimization of the total potential energy of the structural system yields equilibrium equations from which deflections and internal bending moments are determined.

3. Method of superposition of trigonometric series and polynomials shape functions

3.1. General form of the basis functions

In the method of superposition of trigonometric series and polynomial shape functions, the general form of $F_m(x)$ and $G_n(y)$ are:

$$F_m(x) = \sin\left(\frac{m\pi x}{a}\right) + P_m(x) \quad (18a)$$

$$\text{where } P_m(x) = A_{m0} + A_{m1} \left(\frac{x}{a}\right) + A_{m2} \left(\frac{x}{a}\right)^2 + A_{m3} \left(\frac{x}{a}\right)^3 \quad (18b)$$

Hence,

$$F_m(x) = \sin\left(\frac{m\pi x}{a}\right) + A_{m0} + A_{m1} \frac{x}{a} + A_{m2} \frac{x^2}{a^2} + A_{m3} \frac{x^3}{a^3} \quad (19)$$

where $m = 1, 2, 3, 4, 5, \dots$

$$G_n(y) = \sin\left(\frac{n\pi y}{b}\right) + P_n(y) \quad (20a)$$

where $P_n(y) = A_{n_0} + A_{n_1} \left(\frac{y}{b}\right) + A_{n_2} \left(\frac{y}{b}\right)^2 + A_{n_3} \left(\frac{y}{b}\right)^3$ (20b)

Hence,

$$G_n(y) = \sin\left(\frac{n\pi x}{b}\right) + A_{n_0} + A_{n_1} \frac{y}{b} + A_{n_2} \frac{y^2}{b^2} + A_{n_3} \frac{y^3}{b^3}$$
 (21)

where $n = 1, 2, 3, 4, 5, \dots$

$P_m(x)$, $P_n(y)$ are polynomial functions of x and y respectively, $A_{m0}, A_{m1}, A_{m2}, A_{m3}$ are the four coefficients of the polynomial function $P_m(x)$ such that $F_m(x)$ satisfies the plate's boundary conditions at $x = 0$, and $x = a$. $A_{n0}, A_{n1}, A_{n2}, A_{n3}$ are the four coefficients of the polynomial function $P_n(y)$ which are found such that $G_n(y)$ satisfies the plate's boundary conditions at $y = 0$, and $y = b$.

3.2. Basis function coefficients for different support conditions

The boundary conditions depend on the type of restraint along the plate edges $x = 0$, $x = a$, $y = 0$, $y = b$. The following edge support conditions are investigated:

- (i) Simply supported edges at $x = 0$, and $x = a$, and $y = 0$, and $y = b$ (SSSS plate).
- (ii) Edges are simply supported at $x = 0$, clamped at $x = a$, simply supported at $y = 0$, and $y = b$ (SSSC plate).
- (iii) Plate is simply supported at $x = 0$ and clamped at edge $x = a$, simply supported at $y = 0$ and clamped at $y = b$ (SCCS plate).
- (i) Plate is simply supported at $x = 0$, and $x = a$

Figure 3 shows a cross-sectional view of a thin plate simply supported at $x = 0$, and $x = a$.

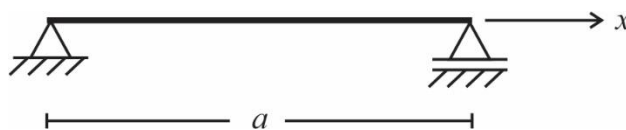


Figure 3: Cross-section of thin plate simply supported at $x = 0$ and $x = a$

The boundary conditions are:

$$F_m(x = 0) = F_m(x = a) = 0$$
 (22)

$$F_m''(x = 0) = F_m''(x = a) = 0$$
 (22)

Applying the boundary conditions,

$$F_m(x = 0) = \sin 0 + A_{m_0} = 0$$
 (23)

$$A_{m_0} = 0$$
 (24)

$$F_m''(x) = -\left(\frac{m\pi}{a}\right)^2 \sin\left(\frac{m\pi x}{a}\right) + 2A_{m_2} \frac{1}{a^2} + 6A_{m_3} \frac{x}{a^3}$$
 (25)

$$F_m''(x = 0) = -\left(\frac{m\pi}{a}\right)^2 \sin 0 + 2A_{m_2} \frac{1}{a^2} = 0$$
 (26)

So, $A_{m_2} = 0$ (27)

$$F_m''(x = a) = \sin(m\pi) + A_{m_1} \left(\frac{a}{a}\right) + A_{m_3} \left(\frac{a^3}{a^3}\right) = 0$$
 (28)

$$\sin(m\pi) + A_{m_1} + A_{m_3} = 0$$
 (29)

$$A_{m_1} + A_{m_3} = -\sin(m\pi) = 0$$
 (30)

$$A_{m_1} = -A_{m_3}$$
 (31)

$$F_m''(x = a) = -\left(\frac{m\pi}{a}\right)^2 \sin(m\pi) + 6A_{m_3} \left(\frac{a}{a^3}\right) = 0$$
 (32)

$$-\left(\frac{m\pi}{a}\right)^2 \sin(m\pi) + \frac{6A_{m_3}}{a^2} = 0 \quad (33)$$

$$A_{m_3} = 0 \quad (34)$$

$$\therefore A_{m_1} = 0 \quad (35)$$

Then,

$$F_m(x) = \sin\left(\frac{m\pi x}{a}\right) \quad (36)$$

Similarly, for plate simply supported at $y=0$, and $y=b$,

$$G_n(y) = \sin\left(\frac{n\pi y}{b}\right) \quad (37)$$

(ii) Kirchhoff plate is simply supported at $x=0$ and clamped at $x=a$

Figure 4 shows a cross-sectional view of thin plate simply supported at $x=0$, and clamped at $x=a$.

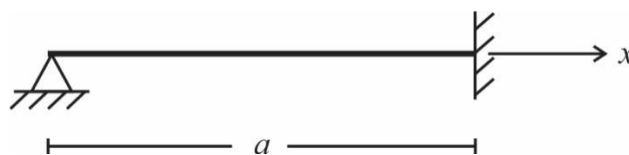


Figure 4: Cross-section of thin plate simply supported at $x=0$, and clamped at $x=a$

The boundary conditions are:

$$F_m(x=0) = 0$$

$$F_m''(x=0) = 0 \quad (38)$$

$$F_m(x=a) = 0$$

$$F_m'(x=a) = 0$$

$$F_m(x=0) = \sin 0 + A_{m_0} = 0 \quad (39)$$

$$A_{m_0} = 0 \quad (40)$$

$$F_m''(x=0) = -\left(\frac{m\pi}{a}\right)^2 \sin 0 + 2A_{m_2} \frac{1}{a^2} = 0 \quad (41)$$

$$A_{m_2} = 0 \quad (42)$$

$$F_m(x=a) = \sin(m\pi) + A_{m_1} + A_{m_3} = 0 \quad (43)$$

$$A_{m_1} + A_{m_3} = 0 \quad (44)$$

$$A_{m_1} = -A_{m_3} \quad (45)$$

$$F_m'(x=a) = \left(\frac{m\pi}{a}\right) \cos(m\pi) + A_{m_1} \left(\frac{1}{a}\right) + 3A_{m_3} \left(\frac{1}{a}\right) = 0 \quad (46)$$

Multiplying by a ,

$$m\pi \cos(m\pi) + A_{m_1} + 3A_{m_3} = 0 \quad (47)$$

From Equation (45) relating A_{m_1} and A_{m_3} ,

$$m\pi \cos(m\pi) - A_{m_3} + 3A_{m_3} = 0 \quad (48)$$

$$2A_{m_3} + m\pi \cos(m\pi) = 0 \quad (49)$$

$$A_{m_3} = -\frac{m\pi \cos(m\pi)}{2} = -\frac{m\pi}{2} (-1)^m \quad (50)$$

$$\text{Then, } A_{m_1} = -A_{m_3} = \frac{m\pi}{2}(-1)^m \quad (51)$$

So,

$$F_m(x) = \sin\left(\frac{m\pi x}{a}\right) + A_{m_1}\left(\frac{x}{a}\right) + A_{m_3}\left(\frac{x^3}{a^3}\right) \quad (52)$$

$$\text{where } A_{m_1} = \frac{m\pi}{2}(-1)^m \quad (53)$$

$$A_{m_3} = -\frac{m\pi}{2}(-1)^m \quad (54)$$

Similarly, for thin plates simply supported at $y = 0$, and clamped at $y = b$,

$$G_n(y) = \sin\left(\frac{n\pi y}{b}\right) + A_{n_1}\left(\frac{y}{b}\right) + A_{n_3}\left(\frac{y^3}{b^3}\right) \quad (55)$$

$$\text{where } A_{n_1} = \frac{n\pi}{2}(-1)^n \quad (56)$$

$$A_{n_3} = -\frac{n\pi}{2}(-1)^n \quad (57)$$

(iii) Plate is clamped at $x = 0$, and simply supported at $x = a$

Figure 5 shows a cross-section of the thin plate clamped at $x = 0$, and simply supported at $x = a$.

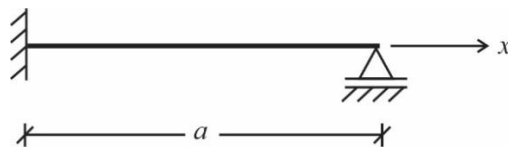


Figure 5: Cross-section of thin plate clamped at $x = 0$, and simply supported at $x = a$

The boundary conditions are:

$$\begin{aligned} F_m(x=0) &= 0 \\ F'_m(x=0) &= 0 \end{aligned} \quad (58)$$

$$\begin{aligned} F_m(x=a) &= 0 \\ F''_m(x=a) &= 0 \end{aligned} \quad (59)$$

$$F_m(x=0) = \sin 0 + A_{m_0} = 0 \quad (60)$$

$$A_{m_0} = 0 \quad (61)$$

$$F'_m(x=0) = \frac{m\pi}{a} \cos 0 + A_{m_1} \frac{1}{a} + 0 = 0 \quad (62)$$

$$\frac{m\pi}{a} + \frac{A_{m_1}}{a} = 0 \quad (63)$$

$$A_{m_1} = -m\pi \quad (64)$$

$$F_m(x=a) = \sin(m\pi) + (-m\pi)\left(\frac{a}{a}\right) + A_{m_2} + A_{m_3} = 0 \quad (65)$$

$$A_{m_2} + A_{m_3} = m\pi - \sin(m\pi) = m\pi \quad (66)$$

$$F''_m(x=a) = -\left(\frac{m\pi}{a}\right)^2 \sin(m\pi) + 2A_{m_2}\left(\frac{1}{a^2}\right) + 6A_{m_3}\left(\frac{a}{a^3}\right) = 0 \quad (67)$$

$$-\frac{(m\pi)^2}{a^2} \sin(m\pi) + \frac{2A_{m_2}}{a^2} + \frac{6A_{m_3}}{a^2} = 0 \quad (68)$$

$$2A_{m_2} + 6A_{m_3} = (m\pi)^2 \sin(m\pi) = 0 \tag{68}$$

$$A_{m_2} + 3A_{m_3} = 0 \tag{69}$$

$$A_{m_2} = -3A_{m_3} \tag{70}$$

Then, substitution of Equation (70) in Equation (65) gives:

$$-3A_{m_3} + A_{m_3} = m\pi \tag{71}$$

$$-2A_{m_3} = m\pi \tag{72}$$

$$A_{m_3} = -\frac{m\pi}{2} \tag{73}$$

Then from Equation (70), we have:

$$A_{m_2} = -3A_{m_3} = \frac{3m\pi}{2} \tag{74}$$

Then,

$$F_m(x) = \sin\left(\frac{m\pi x}{a}\right) + (-m\pi)\left(\frac{x}{a}\right) + \frac{3\pi}{2}\left(\frac{x}{a}\right)^2 + \left(-\left(\frac{m\pi}{2}\right)\left(\frac{x}{a}\right)^3\right) \tag{75}$$

$$F_m(x) = \sin\left(\frac{m\pi x}{a}\right) - m\pi\left(\frac{x}{a}\right) + \frac{3\pi}{2}\left(\frac{x}{a}\right)^2 - \left(\frac{m\pi}{2}\right)\left(\frac{x}{a}\right)^3 \tag{75a}$$

Similarly, for plate clamped at $y = 0$ and simply supported at $y = b$,

$$G_n(y) = \sin\left(\frac{n\pi y}{b}\right) - n\pi\left(\frac{y}{b}\right) + \frac{3\pi}{2}\left(\frac{y}{b}\right)^2 - \frac{ny}{2}\left(\frac{y}{b}\right)^3 \tag{75b}$$

3.3. Ritz variational formulation in terms of $F_m(x)$ and $G_n(y)$

Substitution of the expression for $w(x, y)$ into the Ritz variational functional gives:

$$\begin{aligned} \Pi = \frac{D}{2} \int_0^b \int_0^a \left\{ \left(\nabla^2 \left(\sum_m \sum_n A_{mn} F_m(x) G_n(y) \right) \right)^2 - 2(1-\mu) \left(\frac{\partial^2}{\partial x^2} \left(\sum_m \sum_n A_{mn} F_m(x) G_n(y) \right) \right) \right. \\ \left. \frac{\partial^2}{\partial y^2} \left(\sum_m \sum_n A_{mn} F_m(x) G_n(y) \right) - \left(\frac{\partial^2}{\partial x \partial y} \left(\sum_m \sum_n A_{mn} F_m(x) G_n(y) \right) \right)^2 \right\} dx dy \\ - \int_0^b \int_0^a q(x, y) \sum_m \sum_n A_{mn} F_m(x) G_n(y) dx dy \tag{76} \end{aligned}$$

$$\begin{aligned} \Pi = \sum_m \sum_n A_{mn} \left\{ \frac{D}{2} \int_0^b \int_0^a \left(\nabla^2 F_m(x) G_n(y) \right)^2 - 2(1-\mu) \left[\left(F_m''(x) G_n(y) F_m(x) G_n''(y) \right) \right. \right. \\ \left. \left. - \left(F_m'(x) G_n'(y) \right)^2 \right] \right\} dx dy - \sum_m \sum_n A_{mn} \int_0^b \int_0^a q(x, y) F_m(x) G_n(y) dx dy \tag{77} \end{aligned}$$

3.4. Minimization of the Ritz variational functional

The first variation δ of Π is equal to zero, for a minimum of Π ; which is the equivalent statement of equilibrium of the plate bending problem. Thus,

$$\delta \Pi = 0 \tag{78}$$

The resulting system of algebraic equations become:

$$\sum_m^\infty \sum_n^\infty K_{mn}^{(ij)} A_{mn} = F_{ij} \tag{79}$$

where $K_{mn}^{(ij)}$ is the stiffness matrix, F_{ij} is the force matrix.

$$K_{mn}^{ij} = D \int_0^b \int_0^a \left[\nabla^2 (F_m(x)G_n(y)) \nabla^2 F_i(x)G_j(y) - (1-\mu) (F_m''(x)F_i(x)G_j''(y)G_n(y) + F_i''(x)F_m(x)G_j(y)G_n''(y) - 2F_i'(x)F_m'(x)G_j'(y)G_n'(y)) \right] dx dy \tag{80}$$

$$F_{ij} = \int_0^b \int_0^a q(x, y) F_i(x)G_j(y) dx dy \tag{81}$$

$$K_{mn}^{ij} = D \int_0^b \int_0^a \left[(F_m''(x)G_n(y)F_i''(x)G_j(y) + F_m''(x)G_n(y)F_i(x)G_j''(y) + F_m(x)G_n''(y)F_i''(x)G_j(y) + F_m(x)G_n''(y)F_i(x)G_j''(y)) - (1-\mu) (F_m''(x)F_i(x)G_j''(y)G_n(y) + F_i''(x)F_m(x)G_j(y)G_n''(y) - 2F_i'(x)F_m'(x)G_j'(y)G_n'(y)) \right] dx dy \tag{82}$$

$$K_{mn}^{ij} = D [I_1 I_2 + 2I_3 I_4 + I_5 I_6 - (1-\mu)(2I_3 I_4 - 2I_7 I_8)] \tag{83}$$

For $\mu = 0.30$,

$$K_{mn}^{ij} = D [I_1 I_2 + 2I_3 I_4 + I_5 I_6 - 0.7(2I_3 I_4 - 2I_7 I_8)] \tag{84}$$

$$\begin{aligned} I_1 &= \int_0^a F_m''(x)F_i''(x)dx; & I_2 &= \int_0^b G_n^2(y)dy \\ I_3 &= \int_0^a F_m''(x)F_i(x)dx; & I_4 &= \int_0^b G_n(y)G_j''(y)dy \\ I_5 &= \int_0^a F_m(x)F_i(x)dx; & I_6 &= \int_0^b G_n''(y)G_j''(y)dy \\ I_7 &= \int_0^a F_m'(x)F_i'(x)dx; & I_8 &= \int_0^b G_n'(y)G_j'(y)dy \end{aligned} \tag{85}$$

But $\nabla^2 (F_m(x)G_n(y)) = F_m''(x)G_n(y) + F_m(x)G_n''(y)$ (86)

where $F_m''(x) = \frac{d^2 F_m(x)}{dx^2}$ (87)

$$G_n''(y) = \frac{d^2 G_n(y)}{dy^2} \tag{88}$$

Then,

$$K_{mn}^{ij} = D \int_0^b \int_0^a \left[(F_m''(x)G_n(y) + F_m(x)G_n''(y))(F_i''(x)G_j(y) + F_i(x)G_j''(y)) - (1-\mu) \left((F_m''(x)F_i(x)G_j''(y)G_n(y)) + F_i''(x)F_m(x)G_j(y)G_n''(y) - 2F_i'(x)F_m'(x)G_j'(y)G_n'(y) \right) \right] dx dy \tag{89}$$

When $\mu = 0.30$,

$$K_{mn}^{ij} = D \int_0^b \int_0^a \left[(F_m''(x)G_n(y) + F_m(x)G_n''(y))(F_i''(x)G_j(y) + F_i(x)G_j''(y)) \right]$$

$$\begin{aligned}
 & - 0.7 \left(\left(F_m''(x)F_i(x)G_j''(y)G_n(y) \right) + F_i''(x)F_m(x)G_j(y)G_n''(y) \right. \\
 & \left. - 2F_i'(x)F_m'(x)G_j'(y)G_n'(y) \right) dx dy
 \end{aligned} \tag{90}$$

For uniformly distributed loading, of intensity q_0 ,

$$q(x, y) = q_0 \tag{91}$$

Then,

$$F_{ij} = \int_0^b \int_0^a q_0 F_i(x)G_j(y) dx dy \tag{92}$$

$$F_{ij} = q_0 \int_0^a F_i(x) dx \int_0^b G_j(y) dy = q_0 I_9 I_{10} \tag{93}$$

where,

$$I_9 = \int_0^a F_i(x) dx; \quad I_{10} = \int_0^b G_j(y) dy \tag{94}$$

For hydrostatic distribution of load,

$$q(x, y) = \frac{q_0 x}{a} \tag{95}$$

$$F_{ij} = \int_0^b \int_0^a q_0 \frac{x}{a} F_i(x)G_j(y) dx dy \tag{96}$$

$$F_{ij} = \frac{q_0}{a} \int_0^a x F_i(x) dx \int_0^b G_j(y) dy \tag{97}$$

$$F_{ij} = q_0 \int_0^a \frac{x}{a} F_i(x) dx \int_0^b G_j(y) dy = q_0 I_{11} I_{10} \tag{98}$$

where,

$$I_{11} = \int_0^a \frac{x}{a} F_i(x) dx \tag{99}$$

4. Results

4.1. Results for SSCS Kirchhoff plate bending problem (KPBP)

For KPBP with simple supports at $x = 0, y = 0, y = b$ and clamped edge $x = a$, as shown in Figure 6, $F_m(x)$ and $G_n(y)$ are:

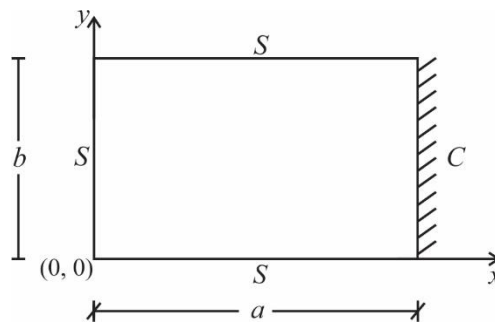


Figure 6: SSCS thin plate

$$F_m(x) = \sin\left(\frac{m\pi x}{a}\right) + A_{m_1}\left(\frac{x}{a}\right) + A_{m_3}\left(\frac{x^3}{a^3}\right) \tag{100}$$

where

$$A_{m_1} = \frac{m\pi}{2}(-1)^m \tag{101}$$

$$A_{m_3} = -\frac{m\pi}{2}(-1)^m$$

$$G_n(y) = \sin\left(\frac{n\pi y}{b}\right); \quad G_j(y) = \sin\left(\frac{j\pi y}{b}\right) \tag{102}$$

$$F_i(x) = \sin\left(\frac{i\pi x}{a}\right) + A_{i_1}\left(\frac{x}{a}\right) + A_{i_3}\left(\frac{x^3}{a^3}\right) \tag{103}$$

$$A_{i_1} = \frac{i\pi}{2}(-1)^i, \quad A_{i_3} = -\frac{i\pi}{2}(-1)^i \tag{104}$$

$$F'_m(x) = \frac{m\pi}{a} \cos\left(\frac{m\pi x}{a}\right) + A_{m_1}\left(\frac{1}{a}\right) + 3A_{m_3}\left(\frac{x^2}{a^3}\right) \tag{105}$$

$$F''_m(x) = -\left(\frac{m\pi}{a}\right)^2 \sin\left(\frac{m\pi x}{a}\right) + 6A_{m_3}\left(\frac{x}{a^3}\right) \tag{106}$$

$$G''_n(y) = -\left(\frac{n\pi}{b}\right)^2 \sin\left(\frac{n\pi y}{b}\right) \tag{107}$$

The deflections found as:

$$w(x, y) = \sum_m \sum_n A_{mn} \left(\sin\left(\frac{m\pi x}{a}\right) + A_{m_1}\left(\frac{x}{a}\right) + A_{m_3}\left(\frac{x^3}{a^3}\right) \right) \sin\left(\frac{n\pi y}{b}\right) \tag{108}$$

The center deflection is found as:

$$w\left(x = \frac{a}{2}, y = \frac{b}{2}\right) = \sum_m \sum_n A_{mn} \left(\sin\left(\frac{m\pi}{2}\right) + \frac{A_{m_1}}{2} + \frac{A_{m_3}}{8} \right) \left(\sin\left(\frac{n\pi}{2}\right) \right) \tag{109}$$

Bending moments

The bending moment-deflection relations are used to find the bending moments from the deflections.

$$M_{xx} = -D(w_{xx} + \mu w_{yy}) \tag{110}$$

$$M_{yy} = -D(w_{yy} + \mu w_{xx})$$

$$w_{xx} = \sum_m \sum_n A_{mn} F''_m(x) G_n(y) \tag{111}$$

$$w_{yy} = \sum_m \sum_n A_{mn} F_m(x) G''_n(y)$$

$$w_{xx} = \sum_m \sum_n A_{mn} \left(-\left(\frac{m\pi}{a}\right)^2 \sin\left(\frac{m\pi x}{a}\right) + 6A_{m_3}\left(\frac{x}{a^3}\right) \right) \left(\sin\left(\frac{n\pi y}{b}\right) \right) \tag{112}$$

$$w_{yy} = \sum_m \sum_n A_{mn} \left(-\left(\frac{n\pi}{b}\right)^2 \sin\left(\frac{n\pi y}{b}\right) \right) \left(\sin\left(\frac{m\pi x}{a}\right) + A_{m_1}\left(\frac{x}{a}\right) + A_{m_3}\left(\frac{x^3}{a^3}\right) \right) \tag{113}$$

The bending moments are:

$$M_{xx} = -D \sum_m \sum_n \left\{ A_{mn} \left(-\left(\frac{m\pi}{a}\right)^2 \sin\left(\frac{m\pi x}{a}\right) + 6A_{m_3}\left(\frac{x}{a^3}\right) \right) \left(\sin\left(\frac{n\pi y}{b}\right) \right) \right\}$$

$$+ \mu \left\{ \sin \frac{m\pi x}{a} + A_{m_1} \frac{x}{a} + A_{m_3} \left(\frac{x}{a} \right)^3 \right\} \left(- \left(\frac{n\pi}{b} \right)^2 \sin \frac{n\pi y}{b} \right) \quad (114)$$

The bending moment at the center is:

$$M_{xx} \left(x = a/2, y = b/2 \right) = -D \sum_m \sum_n \left\{ A_{mn} \left(- \left(\frac{m\pi}{a} \right)^2 \sin \left(\frac{m\pi}{2} \right) + \frac{6A_{m_3}}{a^2} \frac{1}{2} \right) \left(\sin \frac{n\pi}{2} \right) + \mu \left(\sin \left(\frac{m\pi}{2} \right) + \frac{A_{m_1}}{2} + \frac{A_{m_3}}{8} \right) \left(- \left(\frac{n\pi}{b} \right)^2 \sin \left(\frac{n\pi}{2} \right) \right) \right\} \quad (115)$$

$$M_{xx}(0.5a, 0.5b) = -D \sum_m \sum_n A_{mn} \left\{ \left(- \left(\frac{m\pi}{a} \right)^2 \sin \left(\frac{m\pi}{2} \right) + \frac{3A_{m_3}}{a^2} \right) \left(\sin \left(\frac{n\pi}{2} \right) \right) + \mu \left(\sin \left(\frac{n\pi}{2} \right) + \frac{A_{m_1}}{2} + \frac{A_{m_3}}{8} \right) \left(- \left(\frac{n\pi}{b} \right)^2 \sin \left(\frac{n\pi}{2} \right) \right) \right\} \quad (116)$$

Similarly, at the center, M_{yy} , is:

$$M_{yy}(0.5a, 0.5b) = -D \sum_m \sum_n A_{mn} \left\{ \left(\sin \left(\frac{m\pi}{2} \right) + \frac{A_{m_1}}{2} + \frac{A_{m_3}}{8} \right) \left(- \left(\frac{n\pi}{b} \right)^2 \sin \left(\frac{n\pi}{2} \right) \right) + \mu \left(- \left(\frac{m\pi}{a} \right)^2 \sin \left(\frac{m\pi}{2} \right) + \frac{3A_{m_3}}{a^2} \right) \left(\sin \left(\frac{n\pi}{2} \right) \right) \right\} \quad (117)$$

The results for deflections and bending moments at the plate center for SSSC KPBP under uniformly distributed loading are shown in Tables 1 and 2, while Table 3 displays the results for center deflections and bending moments of SSSC KPBP under hydrostatic load distribution.

Table 1. Deflections and bending moments at the center of SSSC KPBP under uniformly distributed loading ($\mu = 0.30$)

a/b	Method / Reference	$Dw(x = 0.5a, y = 0.5b)$ qb^4	$M_{xx}(0.5a, 0.5b)$ qb^2	$M_{yy}(0.5a, 0.5b)$ qb^2
2	Present	0.00928 (-0.215%)	0.0481 (2.34%)	0.0947 (0.745%)
	Zhou Ding (1993)	0.00928	0.0481	0.0947
	Timoshenko & Woinowsky-Krieger (1959)	0.0093	0.047	0.094
1.5	Present	0.00644 (0.625%)	0.0486 (1.25%)	0.0695 (0.725%)
	Zhou Ding (1993)	0.00644	0.0486	0.0695
	Timoshenko & Woinowsky-Krieger (1959)	0.0064	0.048	0.069
1.4	Present	0.00576 (-0.69%)	0.0478 (1.70%)	0.0631 (0.159%)
	Zhou Ding (1993)	0.00576	0.0478	0.0631
	Timoshenko & Woinowsky-Krieger (1959)	0.0058	0.047	0.063
1.3	Present	0.00501 (0.2%)	0.0465 (3.33%)	0.0561 (0.179%)
	Zhou Ding (1993)	0.00501	0.0465	0.0561
	Timoshenko &	0.0050	0.045	0.056

	Woinowsky-Krieger (1959)			
1.2	Present	0.0427 (-0.70%)	0.0449 (2.05%)	0.0490 (0%)
	Zhou Ding (1993)	0.0427	0.0449	0.0490
	Timoshenko & Woinowsky-Krieger (1959)	0.043	0.044	0.0490
1.1	Present	0.00351 (0.29%)	0.0425 (1.19%)	0.0415 (1.22%)
	Zhou Ding (1993)	0.00351	0.0425	0.0415
	Timoshenko & Woinowsky-Krieger (1959)	0.0035	0.042	0.041

The terms enclosed in brackets are differences (in percentage) between the present results and exact results by Timoshenko and Woinowsky-Krieger (1959).

Table 2. Deflections and bending moments at the center of SSSC KPBP under uniformly distributed loading ($\mu = 0.30$)

a/b	Method / Reference	$\frac{Dw(0.5a, 0.5b)}{qa^4}$	$\frac{M_{xx}(0.5a, 0.5b)}{qa^2}$	$\frac{M_{yy}(0.5a, 0.5b)}{qa^2}$
1	Present	0.00279 (-0.36%)	0.0395 (1.28%)	0.0342 (0.59%)
	Zhou Ding (1993)	0.00279	0.0395	0.0342
	Timoshenko & Woinowsky-Krieger (1959)	0.0028	0.039	0.034
1/1.1	Present	0.00317 (-0.94%)	0.0436 (1.40%)	0.0335 (1.51%)
	Zhou Ding (1993)	0.00317	0.0436	0.0335
	Timoshenko & Woinowsky-Krieger (1959)	0.0032	0.043	0.033
1/1.2	Present	0.00350 (0%)	0.0473 (0.64%)	0.0325 (1.56%)
	Zhou Ding (1993)	0.00350	0.0473	0.0325
	Timoshenko & Woinowsky-Krieger (1959)	0.00350	0.047	0.032
1/1.3	Present	0.00380 (0%)	0.0502 (0.4%)	0.0314 (1.29%)
	Zhou Ding (1993)	0.00380	0.0502	0.0314
	Timoshenko & Woinowsky-Krieger (1959)	0.0038	0.050	0.031
1/1.4	Present	0.00404 (1%)	0.0526 (1.15%)	0.0302 (0.67%)
	Zhou Ding (1993)	0.00404	0.0526	0.0302
	Timoshenko & Woinowsky-Krieger (1959)	0.0040	0.052	0.030
1/1.5	Present	0.00424 (0.95%)	0.0547 (1.30%)	0.0290 (3.57%)
	Zhou Ding (1993)	0.00424	0.0547	0.0290
	Timoshenko & Woinowsky-Krieger (1959)	0.0042	0.054	0.028

0.5	Present	0.00489 (-0.20%)	0.0606 (1%)	0.0243 (5.65%)
	Zhou Ding (1993)	0.00489	0.0606	0.0243
	Timoshenko & Woinowsky-Krieger (1959)	0.0049	0.060	0.023

Table 3. Deflections and bending moments at the center of SSSC KPBP under hydrostatic load distribution for $\mu = 0.30$

a/b	Method / Reference	$w(0.5a, 0.5b)$	$M_{xx}(0.5a, 0.5b)$	$M_{yy}(0.5a, 0.5b)$
0.5	Present	$0.00221 q_0 a^4 / D$ (-3.91%)	$0.0285 q_0 a^2$ (1.72%)	$0.0113 q_0 a^2$ (18.18%)
	Zhou Ding (1993)	$0.00221 q_0 a^4 / D$	$0.0285 q_0 a^2$	$0.0113 q_0 a^2$
	Timoshenko & Woinowsky-Krieger (1959)	$0.0023 q_0 a^4 / D$	$0.029 q_0 a^2$	$0.011 q_0 a^2$
$2/3$	Present	$0.00193 q_0 a^4 / D$ (1.58%)	$0.0259 q_0 a^2$ (-0.38%)	$0.0134 q_0 a^2$ (3.08%)
	Zhou Ding (1993)	$0.00193 q_0 a^4 / D$	$0.0259 q_0 a^2$	$0.0134 q_0 a^2$
	Timoshenko & Woinowsky-Krieger (1959)	$0.0019 q_0 a^4 / D$	$0.026 q_0 a^2$	$0.013 q_0 a^2$
1	Present	$0.00129 q_0 a^4 / D$ (-0.77%)	$0.0190 q_0 a^2$ (0%)	$0.0160 q_0 a^2$ (0%)
	Zhou Ding (1993)	$0.00129 q_0 a^4 / D$	$0.0190 q_0 a^2$	$0.0160 q_0 a^2$
	Timoshenko & Woinowsky-Krieger (1959)	$0.0013 q_0 a^4 / D$	$0.019 q_0 a^2$	$0.016 q_0 a^2$
1.5	Present	$0.00304 q_0 b^4 / D$ (1.33%)	$0.0241 q_0 b^2$ (-3.21%)	$0.0331 q_0 b^2$ (2.65%)
	Zhou Ding (1993)	$0.00304 q_0 b^4 / D$	$0.0271 q_0 b^2$	$0.0331 q_0 b^2$
	Timoshenko & Woinowsky-Krieger (1959)	$0.0030 q_0 b^4 / D$	$0.028 q_0 b^2$	$0.034 q_0 b^2$
2	Present	$0.00447 q_0 b^4 / D$ (0.67%)	$0.0242 q_0 b^2$ (0.83%)	$0.0459 q_0 b^2$ (-0.22%)
	Zhou Ding (1993)	$0.00447 q_0 b^4 / D$	$0.0242 q_0 b^2$	$0.0459 q_0 b^2$

Timoshenko & Woinowsky-Krieger (1959)	$0.0045q_0b^4/D$	$0.024q_0b^2$	$0.046q_0b^2$
---	------------------	---------------	---------------

4.2. Results for SCCS Kirchhoff plate bending problem (KPBP)

For KPBP with SCCS boundaries, which is shown in Figure 7, $F_m(x)$ and $G_n(y)$ are given by:

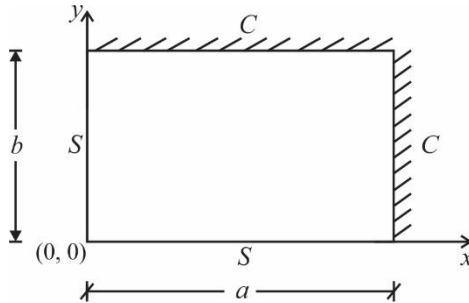


Figure 7: SCCS Kirchhoff plate

$$F_m(x) = \sin\left(\frac{m\pi x}{a}\right) + A_{m1} \frac{x}{a} + A_{m3} \left(\frac{x}{a}\right)^3 \tag{118}$$

$$G_n(y) = \sin\left(\frac{n\pi y}{b}\right) + A_{n1} \frac{y}{b} + A_{n3} \left(\frac{y}{b}\right)^3 \tag{119}$$

Then,

$$w(x, y) = \sum_m \sum_n A_{mn} \left(\sin\left(\frac{m\pi x}{a}\right) + A_{m1} \left(\frac{x}{a}\right) + A_{m3} \left(\frac{x}{a}\right)^3 \right) \left(\sin\left(\frac{n\pi y}{b}\right) + A_{n1} \left(\frac{y}{b}\right) + A_{n3} \left(\frac{y}{b}\right)^3 \right) \tag{120}$$

$$w(x = 0.5a, y = 0.5b) = \sum_m \sum_n A_{mn} \left(\sin\left(\frac{m\pi}{2}\right) + \frac{A_{m1}}{2} + \frac{A_{m3}}{8} \right) \left(\sin\left(\frac{n\pi}{2}\right) + \frac{A_{n1}}{2} + \frac{A_{n3}}{8} \right) \tag{121}$$

$$M_{xx}(0.5a, 0.5b) = -D \sum_m \sum_n A_{mn} \left\{ \left(\frac{3A_{m3}}{a^2} - \left(\frac{m\pi}{a}\right)^2 \sin\left(\frac{n\pi}{2}\right) \right) \left(\sin\left(\frac{n\pi}{2}\right) + \frac{A_{n1}}{2} + \frac{A_{n3}}{8} \right) + \mu \left(\sin\left(\frac{m\pi}{2}\right) + \frac{A_{m1}}{2} + \frac{A_{m3}}{8} \right) \left(\frac{3A_{n3}}{b^2} - \left(\frac{n\pi}{b}\right)^2 \sin\left(\frac{m\pi}{2}\right) \right) \right\} \tag{122}$$

$$M_{yy}(0.5a, 0.5b) = -D \sum_m \sum_n A_{mn} \left\{ \left(\frac{3A_{m3}}{b^2} - \left(\frac{n\pi}{b}\right)^2 \sin\left(\frac{m\pi}{2}\right) \right) \left(\sin\left(\frac{m\pi}{2}\right) + \frac{A_{m1}}{2} + \frac{A_{m3}}{8} \right) + \mu \left(\frac{3A_{n3}}{a^2} - \left(\frac{m\pi}{a}\right)^2 \sin\left(\frac{n\pi}{2}\right) \right) \left(\sin\left(\frac{n\pi}{2}\right) + \frac{A_{n1}}{2} + \frac{A_{n3}}{8} \right) \right\} \tag{123}$$

The results for $w(0.5a, 0.5b)$ and $M_{xx}(0.5a, 0.5b)$, $M_{yy}(0.5a, 0.5b)$ are presented for SCCS thin plates under uniformly distributed loading in Equations (121), (122) and (123). Tables 4 and 5 show the present results center deflection and bending moments of SCCS plates.

Table 4. Deflections and bending moments in SCCS square KPBP under uniformly distributed load ($\mu = 0.30$)

b/a	Reference / Method	$w_c / \left(\frac{qa^4}{D} \right)$	$M_{xx} / (qa^2)$	$M_{yy} / (qa^2)$
1	Present	0.0021040	0.0304	0.0304
	Al-Ali (2016)	0.00210364	0.0304254	0.0304285
	Timoshenko and Woinowsky-Krieger	0.00230	0.0304	0.0304

Table 5. Deflections and bending moments in SCCS rectangular KPBP under uniformly distributed load ($\mu = 0.30$)

b/a	Method / Reference	$w_c / \left(\frac{qa^4}{D} \right)$	$M_{xx} / (qa^2)$	$M_{yy} / (qa^2)$
0.5	Present	0.00295	0.00624	0.0146
	Al-Ali (2016)	0.0029493	0.00624311	0.0146149
0.75	Present	0.0011	0.0172	0.0251
	Al-Ali (2016)	0.00106057	0.0172099	0.0251479
1	Present	0.0021040	0.0304	0.0304
	Al-Ali (2016)	0.00210364	0.0304254	0.0304285
4/3	Present	0.00335	0.0448	0.0306
	Al-Ali (2016)	0.00335123	0.0448045	0.0306366
2	Present	0.0047	0.0591	0.025
	Al-Ali (2016)	0.00468565	0.0590626	0.0249673

5. Discussion

This work has presented the flexural analysis of rectangular Kirchhoff SSSC and SCCS plates subjected to uniformly distributed load, and hydrostatic load distribution using the Ritz variational method (RVM). The important feature of this work is that the basis functions are derived using a superposition of sine functions and third degree polynomial functions, with the four polynomial constants determined such that the boundary conditions are satisfied.

The small displacement assumptions of Kirchhoff plate theory are used in the Ritz formulation to obtain the total potential energy functional; which is minimized with respect to the parameters of the displacement.

Tables 1, 2, and 3 which display the present results and earlier results by Zhou Ding (1993) and Timoshenko and Woinowsky-Krieger (1959) show that the results for center deflections and bending moments are in agreement with previous results of Zhou Ding (1993), and Timoshenko and Woinowsky-Krieger (1959).

Tables 4 and 5 which show the present results for center deflections and bending moments for SCCS square and rectangular plates at various values of b/a ranging from 0.5 to 2 and the corresponding previous result by Al-Ali (2016) confirm that the present results are in close agreement with previous polynomial solutions results by Al-Ali (2016).

Table 1 presents the deflections and bending moments at the center of SSSC KPBT under uniformly distributed load for $a/b = 1, 1.5, 1.4, 1.3, 1.2$ and 1.1 and compares the present results with Zhou Ding (1993) and the exact results of Timoshenko and Woinowsky-Krieger (1959). Table 1 illustrates that for $a/b = 2$, the center deflection obtained in the present study differ from the exact results by Timoshenko and Woinowsky-Krieger (1959) by -0.215% . The differences between the present results and the exact Timoshenko and Woinowsky-Krieger (1959) results vary between -0.215% for $a/b = 2$ to 0.29% for $a/b = 1.1$.

Similarly, the present results for center bending moments M_{xx} differ from the exact value by 3.34% for $a/b = 2$, 1.25% for $a/b = 1.5$, 1.70% for $a/b = 1.4$, 3.33% for $a/b = 1.3$, 2.05% for $a/b = 1.2$ and 1.19% for $a/b = 1.1$. The differences calculated for center bending moments M_{yy} are smaller. Center bending moments M_{yy} differ from the exact value by 0.745% for $a/b = 2$, 0.725% for $a/b = 1.5$, 0.159% for $a/b = 1.4$, 0.179% for $a/b = 1.3$, 0% for $a/b = 1.2$ and 1.22% for $a/b = 1.1$.

Table 2 compares the present results with results by Zhou Ding (1993) and Timoshenko and Woinowsky-Krieger (1959) for center deflections and center bending moments in SSSC KPBP under uniformly distributed load for $a/b = 1, 1/1.1, 1/1.2, 1/1.3, 1/1.4, 1/1.5$ and $1/2$.

Table 2 further shows that the present center deflection results differ from the exact Timoshenko and Woinowsky-Krieger (1959) results by -0.36% for $a/b = 1$, -0.94% for $a/b = 1/1.1$, 0% for $a/b = 1/1.2$, and $a/b = 1/1.3$, 1% for $a/b = 1/1.4$, 0.95% for $a/b = 1/1.5$ and -0.2% for $a/b = 1/2$.

Center bending moments M_{xx} of present study differ from the exact Timoshenko and Woinowsky-Krieger (1959) results by 1.28% for $a/b = 1$ to 1% for $a/b = 0.5$. Center bending moment M_{yy} of present study differ from the exact results of Timoshenko and Woinowsky-Krieger (1959) by various percentages ranging from 0.59% for $a/b = 1$ to 5.65% for $a/b = 0.5$.

Table 3 compares the present results for SSSC KPBP under hydrostatic load for $\mu = 0.30$ with previous results by Zhou Ding and Timoshenko and Woinowsky-Krieger (1959) who presented exact solutions. Table 3 illustrated that the present results for center deflections differ from the exact results by -3.91% for $a/b = 0.5$, 1.58% for $a/b = 2/3$ and 0.67% for $a/b = 2$.

The center bending moments M_{xx} also differ from the exact results by 1.72% for $a/b = 0.5$ to 0.83% for $a/b = 2$. Center bending moments M_{yy} differ from the exact results by 18.18% for $a/b = 2$. Table 3 further shows that the present results are identical to results by Zhou Ding (1993).

Table 4 presents comparison of present results for SCCS square KPBP under uniformly distributed load with previous results by Al-Ali (2016) and Timoshenko and Woinowsky-Krieger (1959). Table 4 shows that the present results are remarkably close to the previous results by Al-Ali (2016) and Timoshenko and Woinowsky-Krieger (1959).

Table 5 compares the present results for SCCS rectangular KPBP under uniformly distributed load with results by Al-Ali (2016) who used polynomial shape functions. Table 5 illustrates that there are negligible differences between the present results and results by Al-Ali (2016) for SCCS KPBP under uniform loading.

6. Conclusion

In this work, the Ritz variational method has been used for the analysis of thin rectangular plate bending problems with adjacent edges clamped and simply supported. The deflection functions used were derived by the superposition of trigonometric series and algebraic polynomial functions such that the geometric and force boundary conditions of the plate bending problems were satisfied.

In conclusion,

- (i) The method of superposition of trigonometric series and polynomial basis functions in the Ritz variational method has been presented in a first principles, rigorous manner and shown to give accurate analytical solutions to the bending problems of SSSC plate under uniformly and hydrostatically distributed loads over the domain and SCCS plate under uniformly distributed load.
- (ii) The basis functions used for the plate bending problems are derived to satisfy the clamped-simply supported boundary conditions in the x -direction and the simply supported boundary conditions in the y -direction, for the SSSC thin plate problem.
- (iii) The basis functions for the SCCS thin plate were constructed to satisfy the simply supported-clamped boundary conditions in the x and y directions respectively.
- (iv) The obtained shape functions are then used to perform a minimization of the obtained Ritz total potential energy functional to give equivalent equilibrium equations for the bending plate.
- (v) The solutions for center deflections and center bending moments in SSSC problem are identical with solutions obtained by Zhou Ding (1993) who used a variant of this method, and Timoshenko and

Woinowsky-Krieger (1959) who used the Levy single series method.

- (vi) The present solutions for center deflections and center bending moments for SCCS KPBP under uniform load are close to the equivalent solutions obtained using a polynomial solution by Al-Ali (2016).

References

- Al-Ali, A.A. (2016). Accurate polynomial solutions for bending of plates with different geometries, loadings and boundary conditions. Master of Science Thesis in Civil Engineering, King Faud University of Petroleum and Minerals, Dhahran, Saudi Arabia.
- Arnold, D.N., Brezzi, F., Marini L.D. (2005). A Family of Discontinuous Galerkin Finite Elements for Reissner-Mindlin plate. *Journal of Scientific Computing* 22, 23; 25 – 45, 2005. DOI: 10.1007/s10915-004-4134-8.
- Du, W., Zhao, X., Hou, H. (2022). A new meshless approach for bending analysis of thin plates with arbitrary shapes and boundary conditions. *Frontiers Structural Civil Engineering*, 16, 75 – 85. <https://doi.org/10.1007/s11709-021-0798-5>
- Fogang, V. (2023). Another approach to the analysis of isotropic rectangular thin plates subjected to external bending moments using the Fourier series. www.preprints.org doi.10.20944/preprints.20230700112v2.
- Hansbo, P., Larson, M.G. (2017). Continuous/discontinuous finite element modelling of Kirchhoff plate structures in R^3 using tangential differential calculus. *Computational Mechanics* (2017) 60: 693 – 702. DOI: 10.1007/s00466-017-1431-2.
- Gao, J., Dang, F., Ma, Z., Ren, J. (2019). Deformation and mechanical behaviors of SCSF and CCCF rectangular thin plates loaded by hydrostatic pressure. *Advances in Civil Engineering*, 2019, Article ID:1560171, 12 pages. <https://doi.org/10.1155/2019/1560171>.
- Ghugal, Y.M., Gajbhiye, P.D. (2016). Bending analysis of thick isotropic plates by using 5th order shear deformation theory. *Journal of Applied and Computational Mechanics*, 2(2), 80 – 95.
- Ghugal, Y.M., Sayyad, A.S. (2010). A static flexure of thick isotropic plates using trigonometric shear deformation theory. *Journal of Solid Mechanics*, 2(1), 79 – 90.
- Goloskokov, D.P., Matrosov, A.V. (2017). Analysis of elastic systems with discontinuous parameters. 2017 Constructive Nonsmooth Analysis and Related Topics (dedicated to the memory of V.F. Demyanov) CNSA St Petersburg, Russia, 2017, 1 – 4. DOI: 10.1109/CNSA/2017.7973959.
- Guo, H.W., Zhuang, X.Y., Rabczuk, T. (2019). A deep collocation method for the bending analysis of Kirchhoff plate. *CMC-Computer Materials and Continua*, 59(2), 433 – 456.
- Ibearugbulem, O.M., Ezeh, J.C., Ettu, L.O. (2019). Pure bending analysis of thin rectangular SSSS plate using Taylor-Maclaurin series. *International Journal of Civil and Structural Engineering*, 5(1), 18 – 24.
- Ike, C.C. (2018). Systematic presentation of Ritz variational method for the flexural analysis of simply supported rectangular Kirchhoff-Love plates. *Journal of Engineering Sciences*, 5(2), D1 – D5. DOI:10.21272/jes.2018.5(2).d1
- Ike, C.C. (2021). Generalized integral transform method for bending analysis of clamped rectangular thin plates. *Journal of Computational Applied Mechanics*, 53(4), 599 – 625. DOI:10.22059/JCAMECH.2022.350620.768
- Ike, C.C. (2023). Exact analytical solutions to bending problems of SFrSFr thin plates using variational Kantorovich-Vlasov method. *Journal of Computational Applied Mechanics*, 54(2), 186 – 203. DOI:10.22059/JCAMECH/2023.351563.776
- Ike, C.C., Nwoji, C.U., Mama, B.O., Onah, H.N., Onyia, M.E. (2020). Least squares weighted residual method for finding the elastic stress fields in rectangular plates under uniaxial parabolically distributed edge loads. *Journal of Computational Applied Mechanics*, 51(1), 107 – 121. DOI:10.22059/JCAMECH.2020.298074.484
- Karttunen, A.T., Von Herten, R., Reddy, J.N., Romanoff, J. (2017). Exact elasticity-based finite element for circular plates. *Computers and Structures*, 182, 219 – 226.
- Koc, S. (2023). Trigonometric series solution for analysis of composite laminated plates. MSc Thesis, Middle East Technical University.

- Li, R., Wang, P., Tian, Y., Wang, B., Li, G. (2015). A unified analytic solution approach to static bending and free vibration problems of rectangular thin plates. *Scientific Reports*, 5, 17054. DOI:10.1038/srep.17054
- Lim, C.W., Cui, S., Yao, W.A. (2007). On new symplectic elasticity approach for exact bending solutions of rectangular thin plates with opposite sides simply supported. *International Journal of Solids and Structures*, 44(16), 5396 – 5411. <https://doi.org/10.1016/j.solstr.2007.01.007>
- Lytvyn, O.M., Lytvyn, O.O., Tamanova, I.S. (2018). Solving the biharmonic plate bending problem by the Ritz method using explicit formulas for spheres of degree 5. *Cybern Syst Analy*, 54, 944 – 947. <https://doi.org/10.1007/s10559-018-0097-x>
- Ma, C.M. (2008). Symplectic eigen-solution for clamped Mindlin plate bending problem. *Journal of Shanghai Jiaotong University*, 12(5), 377 – 382.
- Mama, B.O., Nwoji, C.U., Ike, C.C., Onah, H.N. (2017). Analysis of simply supported rectangular Kirchhoff plates by the finite Fourier sine transform method. *International Journal of Advanced Engineering, Research and Science*, 4(3), 285 – 291. <https://dx.doi.org/10.22161/ijaers.4.4.44>
- Mama, B.O., Oguaghamba, O.A., Ike, C.C. (2020). Single finite Fourier sine integral transform method for the flexural analysis of rectangular Kirchhoff plate with opposite edges simply supported, other edges clamped for the case of triangular load distribution. *International Journal of Engineering Research and Technology*, 13(7), 1802 – 1813.
- Mindlin, R.D. (1951). Influence of rotatory inertia and shear deformation on flexural motion of isotropic, elastic plates. *Journal of Applied Mechanics*, 18, 31 – 38.
- Musa, A.E.S., Al-Shugaa, M.A., Al-Gahtani, H.J. (2020). Energy based solution for bending analysis of thin plates on nonhomogeneous elastic foundation. *Arabian Journal of Science and Engineering*, 45(5), 3817 – 3827. <https://doi.org/10.1007/s13369-0119-04255-1>
- Nareen, K., Shimpi, R.P. (2015). Refined hyperbolic shear deformation plate theory. *Proceedings of the Institution of Mechanical Engineers, Part C, Journal of Mechanical Engineering Science*, 229(15), 2675 – 2686. <https://doi.org/10.1177/095440621456373>
- Nwoji, C.U., Mama, B.O., Onah, H.N., Ike, C.C. (2018a). Flexural analysis of simply supported rectangular Mindlin plates under bisinusoidal transverse load. *ARPN Journal of Engineering and Applied Sciences*, 13(15), 4480 – 4488.
- Nwoji, C.U., Onah, H.N., Mama, B.O., Ike, C.C. (2018b). Theory of elasticity formulation of the Mindlin plate equations. *International Journal of Engineering and Technology*, 9(6), 4344 – 4352. DOI:10.21817/ijet/2017/v9i6/170906074
- Nwoji, C.U., Onah, H.N., Mama, B.O., Ike, C.C. (2018c). Ritz variational methods for bending of rectangular Kirchhoff-Love plate under transverse hydrostatic load distribution. *Mathematical Modelling of Engineering Problems*, 5(1), 1 – 10. <https://doi.org/10.18280/mmep.050101>
- Oba, E.C., Anyadiegwu, P.C., George, A.G.T., Nwadike, E.C. (2018). Pure bending analysis of isotropic thin rectangular plates using third-order energy functional. *International Journal of Scientific and Research Publication*, 8(3), 254 – 262. <https://dx.doi.org/10.29322/IJSRP.8.3.2018p.7537>
- Onah, H.N., Mama, B.O., Ike, C.C., Nwoji, C.U. (2017). Kantorovich-Vlasov method for the flexural analysis of Kirchhoff plates with opposite edges clamped and simply supported (CSCS plates). *International Journal of Engineering and Technology*, 9(6), 4333 – 4343. DOI:10.21817/ijet/2017v9i6/170906073
- Onah, H.N., Onyia, M.E., Mama, B.O., Nwoji, C.U., Ike, C.C. (2020). First principles derivation of displacement and stress function for three-dimensional elastostatic problems, and application to the flexural analysis of thick circular plates. *Journal of Computational Applied Mechanics*, 51(1), 184 – 198. DOI:10/22059/JCAMECH
- Osadebe, N.N., Ike, C.C., Onah, H., Nwoji, C.U., Okafor, F.O. (2016). Application of Galerkin-Vlasov method to the flexural analysis of simply-supported rectangular Kirchhoff plates under uniform loads. *Nigerian Journal of Technology*, 35(4), 732 – 738. <https://doi.org/10.4314/nijt.v35i46>
- Reddy, J.N. (1984). A refined non-linear theory of plates with transverse shear deformation. *International Journal of Solids and Structures*, 20, 881 – 896.
- Reissner, E. (1945). The effect of transverse shear deformation on the bending of elastic plates. *Journal of Applied Mechanics*, 3, 69 – 77.

- Rezaiee-Pajand, M., Karkon, M. (2014). Hybrid stress and analytical functions for analysis of thin plates bending. *Latin American Journal of Solids and Structures*, 11(2014), 556 – 579.
- Rouzegeer, J., Abdoli-Sharifpoor, R. (2015). A finite element formulation for bending analysis of isotropic and orthotropic plates based on two-variable refined plate theory. *Scientia Iranica Transactions B Mechanical Engineering*, 22(1), 196 – 207.
- Shakir, Q.M., Alliwe, R. (2020). Upgrading of deficient disturbed regions in precast RC beams with near surface mounted (NSM) steel bars. *Journal of Materials and Engineering Structures* 7(2002), 167 – 184.
- Shakir, Q.M., Farooq alghazali, A. (2023). New model of eco-friendly hybrid deep beams with wastes of crushed concrete. *Jurnal Teknolgi* 85(6), 145 – 154. <https://doi.org/10.11113/jurnal.teknoligi.v85.20431>.
- Shakir, Q.M., Hanoon, H.K. (2023). New models for reinforced concrete precast hybrid deep beams under static loads with curved hybridization. *Structures* 54, 1007 – 1025. <https://doi.org/10.1016/j.struct.2023.05.084>.
- Shakir, Q.M., Hanoon, H.K. (2024). Innovative model of precast RC curved hybrid deep beams composed partially with high-performance concrete. *Arabian Journal for Science and Engineering* 49(2024), 6045 – 6060. <https://doi.org/10.1007/s13369-023-08592-0>.
- Shakir, Q.M., Yahya, Y.M. (2024). Stitching of T-deep beams with large openings by CFRP sheets and NSM steel bars. *Pollack Periodica*. DOI: 10.1556/606.2024.00979.
- Soltani, K., Bassaim, A., Houari, M.S.A., Kaci, A., Benguediab, M., Tounsi, A., Alhodaly, M.Sh. (2019). A novel hyperbolic shear deformation theory for the mechanical buckling analysis of advanced composite plates resting on elastic foundations. *Steel and Composite Structures*, 30(1), 13 – 29. <https://doi.org/10.2989/scs.2019.30.1.013>
- Shuang, C. (2007). *Symplectic elasticity approach for exact bending solution of rectangular thin plates*. Master of Philosophy Thesis, City University of Hong Kong.
- Su, X., Bai, E., Hai, G. (2023). Unified solution of some problems of rectangular plates with four free edges based on symplectic superposition method. *Engineering Computations*. <https://doi.org/10.1108/EC-08-2022-0533>
- Timoshenko, S.P., Woinowsky-Krieger, S. (1959). *Theory of Plates and Shells*, 2nd Edition, McGraw-Hill, New York.
- Wang, B., Li, P., Li, R. (2016). Symplectic superposition method for new analytical buckling solutions of rectangular thin plates. *International Journal of Mechanical Sciences*, 119(2016), 432 – 441.
- Xia, F., Li, S. (2021). R-function and variation method for bending problem of clamped thin plate with complex shape. *Advances in Mechanical Engineering*, 13(7). <https://doi.org/10.1177/16878140211034832>
- Zerfu, K., Ekaputri, J.J. (2017). An approximate deflection function for simply supported quadrilateral thin plate by variational approach. *AIP Conference Proceedings*, 020014. <https://doi.org/10.1068/1.4994417>
- Zheng, X., Huang, M., An, D., Zhou, C., Li, R. (2021). New analytic bending buckling, and free vibration solutions of rectangular nanoplates by the symplectic superposition method. *Scientific Reports*, 2021, 11:2939. <https://doi.org/10.1038/s41598-021-82326-w>
- Zhong, Y., Li, R. (2009). Exact bending analysis of fully clamped rectangular thin plates subjected to arbitrary loads by new symplectic elasticity approach. *Research Communications*, 36(6), 707 – 714.
- Zhou Ding (1993). An approximate solution with high accuracy of transverse bending of thin rectangular plates under arbitrary distributed loads. *Applied Mathematics and Mechanics*, 14(3), 241 – 246.